Impacts of Risk Metrics for Wildfire-Driven Public Safety Power Shutoffs

Caoyang Cheng, *Student Member, IEEE*, Junbo Zhao, *Senior Member, IEEE*

***Abstract*—Public safety power shutoffs (PSPS) force utilities to identify trade-off between wildfire ignition safety and service continuity, yet the operative meaning of wildfire risk is often unclear. In this paper, how different risk metrics shape PSPS strategies is assessed. The optimal PSPS strategy is formulated as a risk-constrained unit commitment problem. Two risk indices are introduced to assess their impacts on PSPS, including the geographic exposure using the Wildland Fire Potential Index (WFPI) and a consequence-weighted index (WGR) proportional to expected unserved energy from a probabilistic wildfire ensemble. A cross-evaluation algorithm is proposed, where for each risk tolerance, one risk index is first evaluated, and the resulting plan under both metrics is further assessed. This allows comprehensive quantifications of different risk metric impacts. The numerical results tested on the modified RTS–GMLC system show that the choice of risk metric materially changes PSP strategies. At 0% risk tolerance, the plans disagree on 76.9% of line statuses. Across 0–40% tolerance, WGR reduces total operating cost by 40–50% while matching or improving reliability (up to 2.1% of demand served) by preserving backbone transfers and allocating permitted exposure to redundant corridors.**

***Index Terms*—Public safety power shutoffs, wildfire risk assessment, transmission system resilience, optimization**

I. Introduction

The increasing frequency and severity of wildfire events on electric infrastructure have affected power system operations in fire-prone regions. California's devastating Camp Fire (2018) and the Dixie Fire (2021), are both attributed to utility equipment failures, exemplifying the catastrophic consequences when energized infrastructure interacts with extreme weather conditions. In response, utilities have adopted *Public Safety Power Shutoffs* (PSPS) as an emergency measure to preemptively de-energize transmission and distribution lines during periods of elevated fire danger. While PSPS events can effectively reduce ignition probability, they impose substantial reliability penalties and socioeconomic costs on affected communities, particularly critical services, such as hospitals, water treatment facilities, and communication infrastructure [1]–[3].

The operational challenge for system operators is multifaceted: how to systematically balance wildfire prevention against service continuity in a manner that is both technically sound and socially defensible. This challenge becomes particularly acute when considering that PSPS decisions must be made under significant uncertainty regarding weather conditions, fire behavior, and system response, while maintaining transparency for regulatory oversight and public accountability.

Substantial research has addressed the technical aspects of PSPS implementation through various optimization frameworks. These include transmission topology control for resilience enhancement, security-constrained unit commitment with detailed ramping constraints, and advanced resilience strategies incorporating microgrids and intentional islanding capabilities [4]–[7]. The predominant approach in current PSPS literature follows a *geographic-exposure* paradigm, where geospatial fire-danger indicators—most notably the U.S. Geological Survey's *Wildland Fire Potential Index* (WFPI)—are mapped onto transmission corridors to create line-level risk weights. The resulting optimization model minimizes the aggregate geographic exposure subject to operational constraints [8], [9]. Concurrently, the power systems resilience community has developed sophisticated approaches emphasizing *system consequences* rather than geographic hazards alone. This perspective prioritizes components based on their impact on service continuity and potential cascading failures, naturally connecting to risk-aware optimal power flow employing chance constraints or coherent risk measures [2], [3], [10], [11]. These consequence-based approaches recognize that not all transmission corridors contribute equally to system reliability, where some form a critical backbone infrastructure while others provide redundant capacity. Despite the coexistence of these paradigms, their comparative implications for PSPS decision-making remain unexplored. Each approach embodies distinct value judgments about acceptable risk and implicitly traces different feasible regions for operational decisions.

This paper develops a unified PSPS planning framework in which the physical network model, operational constraints, and solution algorithm are fixed while only the wildfire risk metric varies. Within a single risk-constrained unit commitment formulation, this paper compares a WFPI-based metric that penalizes energizing lines in high-hazard areas with a consequence-weighted WGR metric derived from probabilistic wildfire scenarios, which assigns higher weights to corridors whose failure would cause greater expected unserved energy. For each risk tolerance level, this paper solves the optimization under one metric and then evaluates the resulting plan under both metrics, enabling a fair comparison of how the two risk definitions allocate permitted exposure across the RTS-GMLC test system [12].

This work is partially supported by The Arthur L. Irving Institute for Energy & Society at Dartmouth College and U.S. Department of Energy Office of Cybersecurity, Energy Security, and Emergency Response.

C. Cheng and J. Zhao are with the Thayer School of Engineering, Dartmouth College, Hanover, NH 03755, USA (e-mail: caoyang.cheng.TH@dartmouth.edu, junbo.zhao@dartmouth.edu).

979-8-3315-8138-1

II. Problem Formulation

The PSPS planning problem is formulated as a risk-constrained unit commitment with DC network constraints and topology control. For each transmission corridor $(i,j) \in \mathcal{L}$, let $z_{ij,t} \in \{0,1\}$ denote the *energization* status at time t ($z_{ij,t} = 1$ if energized, 0 if de-energized); if a de-energization indicator $x_{ij,t}$ is preferred as in the opening sentence, it satisfies $x_{ij,t} = 1 - z_{ij,t}$. Generators $g \in \mathcal{G}$ have binary commitment $z_{g,t} \in \{0,1\}$, start-up/shutdown indicators $z_{g,t}^{\mathrm{up}}, z_{g,t}^{\mathrm{dn}} \in \{0,1\}$, and continuous output $p_{g,t} \geq 0$. Loads $d \in \mathcal{D}$ have a served fraction $x_{d,t} \in [0,1]$ applied to the nominal demand $p_{d,t}$ so that $(1 - x_{d,t})p_{d,t}$ is the curtailed energy valued at C_d^{VoLL}. Line flows $p_{ij,t}$ and bus angles $\theta_{i,t}$ follow the DC model with susceptance B_{ij}; $\underline{\theta}, \overline{\theta}$ are big-M bounds that decouple angles when a line is off. Wildfire risk enters via nonnegative weights $R_{ij,t} \geq 0$ and a per-period budget R_{tol} with a slack $R_{\mathrm{slack}} \in [0, \overline{R}_{\mathrm{slack}}]$.

Objective and cost decomposition: The objective

$$C^{\mathrm{total}} = C^{\mathrm{uc}}\big(\boldsymbol{z}_g^{\mathrm{up}}, \boldsymbol{z}_g^{\mathrm{dn}}\big) + C^{\mathrm{oc}}\big(\boldsymbol{p}_g\big) + C^{\mathrm{VoLL}}\big(\boldsymbol{x}_d, \boldsymbol{p}_d\big) + R_{\mathrm{slack}} \tag{1}$$

minimizes four terms: (i) commitment transition cost

$$C^{\mathrm{uc}}\big(\boldsymbol{z}_g^{\mathrm{up}}, \boldsymbol{z}_g^{\mathrm{dn}}\big) = \sum_{t \in \mathcal{T}} \sum_{g \in \mathcal{G}} \big(C_g^{\mathrm{up}}\, z_{g,t}^{\mathrm{up}} + C_g^{\mathrm{dn}}\, z_{g,t}^{\mathrm{dn}}\big), \tag{2}$$

where $C_g^{\mathrm{up}}/C_g^{\mathrm{dn}}$ price start-up/shutdown events; (ii) production cost

$$C^{\mathrm{oc}}\big(\boldsymbol{p}_g\big) = \sum_{t \in \mathcal{T}} \sum_{g \in \mathcal{G}} C_g\, p_{g,t}, \tag{3}$$

with linear marginal cost C_g; (iii) unserved-energy cost

$$C^{\mathrm{VoLL}}\big(\boldsymbol{x}_d, \boldsymbol{p}_d\big) = \sum_{t \in \mathcal{T}} \sum_{d \in \mathcal{D}} C_d^{\mathrm{VoLL}}\,(1 - x_{d,t})\, p_{d,t}, \tag{4}$$

which monetizes load shedding through $x_{d,t}$; and (iv) an explicit penalty R_{slack} for violating the per-period wildfire risk budget. This places operational cost and wildfire exposure on a common economic footing.

Unit-commitment logic: Minimum up/down times and state transitions are enforced by

$$z_{g,t} \geq \sum_{t' = t - t_g^{\mathrm{MinUp}} + 1}^{t} z_{g,t'}^{\mathrm{up}}, \qquad \forall g, t, \tag{5}$$

$$1 - z_{g,t} \geq \sum_{t' = t - t_g^{\mathrm{MinDn}} + 1}^{t} z_{g,t'}^{\mathrm{dn}}, \qquad \forall g, t, \tag{6}$$

$$z_{g,t+1} - z_{g,t} = z_{g,t+1}^{\mathrm{up}} - z_{g,t+1}^{\mathrm{dn}}, \qquad \forall g, t, \tag{7}$$

where $t_g^{\mathrm{MinUp}}/t_g^{\mathrm{MinDn}}$ are the minimum up/down durations. The equality (7) links the binary trajectory $z_{g,t}$ with start-up/shutdown events, ensuring consistency across time.

Output envelope and ramping through transitions: Dispatch $p_{g,t}$ respects status-coupled limits

$$z_{g,t}\, \underline{p}_g \leq p_{g,t} \leq z_{g,t}\, \overline{p}_g, \qquad \forall g, t, \tag{8}$$

so $p_{g,t} = 0$ if $z_{g,t} = 0$ and $p_{g,t} \in [\underline{p}_g, \overline{p}_g]$ otherwise. To keep ramping linear across on/off boundaries, we use the auxiliary trajectory

$$p_{g,t}^{\mathrm{aux}} = p_{g,t} - z_{g,t}\, \overline{p}_g, \qquad \forall g, t, \tag{9}$$

$$\underline{U}_g \leq p_{g,t+1}^{\mathrm{aux}} - p_{g,t}^{\mathrm{aux}} \leq \overline{U}_g, \qquad \forall g, t, \tag{10}$$

with $\underline{U}_g, \overline{U}_g$ the down/up ramp bounds. Because $p_{g,t}^{\mathrm{aux}}$ absorbs the commitment shift by $-\overline{p}_g$, (10) remains valid at start-ups and shutdowns without case-splitting.

PSPS monotonicity for line status: Operationally, once a corridor is de-energized for safety, it cannot be re-energized within the horizon. We enforce this with the nonincreasing constraint

$$z_{ij,t} \geq z_{ij,t+1}, \qquad \forall (i,j) \in \mathcal{L},\ \forall t, \tag{11}$$

which precludes oscillatory switching and captures inspection/recertification delays.

DC power flow with switchable corridors: For each energized line ($z_{ij,t} = 1$), flows and angles obey the standard DC relation $p_{ij,t} = -B_{ij}(\theta_{i,t} - \theta_{j,t})$ and thermal limits; when de-energized ($z_{ij,t} = 0$), the capacity constraint forces $p_{ij,t} = 0$ and the angle coupling is relaxed via big-M bounds:

$$\begin{aligned} p_{ij,t} &\leq -B_{ij}(\theta_{i,t} - \theta_{j,t}) + \overline{\theta}\,\big(1 - z_{ij,t}\big), \\ p_{ij,t} &\geq -B_{ij}(\theta_{i,t} - \theta_{j,t}) + \underline{\theta}\,\big(1 - z_{ij,t}\big), \\ z_{ij,t}\, \underline{p}_{ij} &\leq p_{ij,t} \leq z_{ij,t}\, \overline{p}_{ij}. \end{aligned}$$

Here $\underline{p}_{ij}, \overline{p}_{ij}$ are thermal ratings, and $\underline{\theta}, \overline{\theta}$ are chosen wide enough to deactivate the DC coupling when $z_{ij,t} = 0$. One bus angle per period is set as reference.

System balance: At each period, total generation plus net line injections equals served load,

$$\sum_{g \in \mathcal{G}} p_{g,t} \;+\; \sum_{(i,j) \in \mathcal{L}} p_{ij,t} \;-\; \sum_{d \in \mathcal{D}} x_{d,t}\, p_{d,t} \;=\; 0, \tag{12}$$

where $x_{d,t} p_{d,t}$ is the supplied demand and the middle term sums the oriented line flows.

Wildfire risk budget: Wildfire exposure is limited per period by

$$\sum_{(i,j) \in \mathcal{L}} z_{ij,t}\, R_{ij,t} \;+\; R_{\mathrm{slack}} = R_{\mathrm{tol}}, \qquad \forall\, t \in \mathcal{T}, \tag{13}$$

$$0 \;\leq\; R_{\mathrm{slack}} \;\leq\; \overline{R}_{\mathrm{slack}}, \tag{14}$$

so only *energized* corridors contribute to the budget via weights $R_{ij,t} \geq 0$. The metric $R_{ij,t}$ instantiates either a geographic exposure (e.g., WFPI-based) or a system-consequence weight (e.g., WGR-based); the choice of $R_{ij,t}$ is the only difference between risk paradigms. For reporting, the cumulative exposure is

$$R_{\mathrm{Tot}} = \sum_{t \in \mathcal{T}} \sum_{(i,j) \in \mathcal{L}} z_{ij,t}\, R_{ij,t}. \tag{15}$$

III. Proposed Cross-Evaluation Methodology

We compare two distinct risk concepts within a single PSPS optimization framework. We first build a geographic-exposure metric (WFPI) from terrain and weather, and then the system-consequence metric (WGR) that captures how line failures affect reliability. Finally, the plans produced by each metric are cross-evaluated to isolate how the risk definition shapes operations and outcomes.

A. WFPI: Geographic-Exposure Risk Construction

The Wildland Fire Potential Index (WFPI) provides daily gridded hazard estimates by integrating fuel moisture, wind, and terrain, yielding spatially explicit conditions conducive to large fires.

For each corridor $m \in \mathcal{L}$, we collect the set $\mathcal{I}_m$ of WFPI cells that intersect the corridor or lie within a 1-km buffer (to reflect potential spread). Sampling the corridor at 50-meter intervals, we compute the overlap length $\ell_{i,m}$ (km) with each cell i and form the length-weighted average:

$$r_m^{\mathrm{WFPI}} = \frac{\sum_{i \in \mathcal{I}_m} \mathrm{WFPI}_i \, \ell_{i,m}}{\sum_{i \in \mathcal{I}_m} \ell_{i,m}} \geq 0, \tag{16}$$

Optionally, values are rescaled to $[0,1]$ for numerical consistency while preserving rankings. The PSPS budget constraint is

$$\sum_{(i,j) \in \mathcal{L}} z_{ij,t} \, r_{ij}^{\mathrm{WFPI}} + R_{\text{slack}} = R_{\text{tol}}, \qquad 0 \leq R_{\text{slack}} \leq \overline{R}_{\text{slack}}, \tag{17}$$

which instantiates (13)–(14) for the geographic metric.

B. WGR: System-Consequence Risk Construction

WGR reframes risk as expected system consequence: corridors contribute unequally to reliability, so losing a critical backbone can cause widespread outages, whereas redundant paths provide flexibility.

Using the same spatial discretization, each grid cell i is assigned a scenario-dependent failure probability $\pi_i \in [0,1]$ based on fire intensity, wind, and infrastructure vulnerability. Corridor-level failure propensity is

$$\mathrm{CrtLine}_m = \frac{\sum_{i \in \mathcal{I}_m} \pi_i \, \ell_{i,m}}{\sum_{i \in \mathcal{I}_m} \ell_{i,m}} \in [0,1], \tag{18}$$

which mirrors the WFPI aggregation but incorporates failure likelihood.

A scenario set Ω is constructed, where each scenario ω (with probability P_ω^{wf}) represents an ignition–weather–progression combination calibrated from data. For scenario ω and failure set s, the optimal power flow yields VoLL-weighted unserved energy $\Delta I_{\omega,s}$. The expected consequence and corridor contribution are

$$R^{\mathrm{sys}} = \sum_{\omega \in \Omega} P_\omega^{\mathrm{wf}} \sum_{s} \Big(\prod_{i \in s} p_{\omega,i} \Big) \Delta I_{\omega,s}, \tag{19}$$

$$R_m^{\mathrm{corr}} = R^{\mathrm{sys}} - R^{\mathrm{sys}}\big|_{p_{\omega,m}=0}, \qquad r_m^{\mathrm{WGR}} = \mathrm{norm}\big(R_m^{\mathrm{corr}}\big), \tag{20}$$

where the normalization aligns scales with WFPI while preserving relative importance.

Remark (Information boundary). The WGR construction uses two inputs: (i) a Monte Carlo fire ensemble that stochastically knocks out lines via the spatiotemporal fragility model, and (ii) a contingency-based OPF that evaluates VoLL-weighted unserved energy on the *damaged* network. Crucially, the topology in this offline stage is *not* a decision variable—lines fail exogenously according to fire scenarios. By contrast, the online PSPS optimizer treats topology as an endogenous decision and uses the pre-computed r_m^{WGR} as fixed parameters. This separation—exogenous contingency assessment offline, voluntary de-energization optimization online—mirrors standard practice in N-k security screening and does not constitute circular reasoning.

C. Cross-Evaluation Protocol

Under each index, all modeling elements (structure, constraints, solver) are held fixed; only the risk weight vector $\boldsymbol{r}$ and its budget vary.

To compare across scales, each metric's maximum exposure $R_\star^M = \sum_{(i,j) \in \mathcal{L}} r_{ij}^M$ is normized, and the tolerance $\rho \in [0,100]\%$ is $R_{\text{tol}}^M(\rho) = (\rho/100) R_\star^M$. For each ρ, we solve under both paradigms to obtain x^{WFPI} and x^{WGR}, then evaluate each plan under *both* metrics:

- Total operating cost $C(x)$ (commitment, production, VoLL)
- Service reliability $\eta(x)$ (percent demand served)
- Geographic exposure $E^{\mathrm{WFPI}}(x) = \sum_t \sum_{(i,j)} z_{ij,t}(x) \, r_{ij}^{\mathrm{WFPI}}$
- Consequence exposure $E^{\mathrm{WGR}}(x) = \sum_t \sum_{(i,j)} z_{ij,t}(x) \, r_{ij}^{\mathrm{WGR}}$

We quantify how solutions differ via the fraction of corridors whose status differs at any time:

$$D(\rho) = \frac{1}{|\mathcal{L}|} \sum_{(i,j)} \mathbf{1}[\exists t : \, z_{ij,t}^{\mathrm{WFPI}} \neq z_{ij,t}^{\mathrm{WGR}}] \times 100\% \tag{21}$$

Algorithm 1 formalizes the procedure while we keep its narrative description here minimal.

IV. Numerical Results

The proposed cross-evaluation framework is tested under the RTS-GMLC system [12], which comprises 39 transmission corridors spanning California, Nevada, and Arizona with heterogeneous wildfire exposure. The geographic-exposure metric draws on 1-km resolution WFPI datasets from the U.S. Geological Survey [13]; Fig. 1 maps bus locations and corridor-level WFPI values across the network. The system-consequence metric (WGR) is constructed from 8,000 Monte Carlo wildfire scenarios incorporating spatiotemporal fragility models [14]. All optimization problems are solved using Gurobi 10.0. The WFPI-based and WGR-based optimization are compared across six risk tolerance levels (0%, 20%, 40%, 60%, 80%, 100%), evaluating each resulting plan under both risk metrics.

979-8-3315-8138-1

Algorithm 1 CROSSEVAL: Systematic Comparison Protocol

Require: Network $(\mathcal{G}, \mathcal{L}, \mathcal{T})$, PSPS model (Section II), risk weights $\boldsymbol{r}^{\mathrm{WFPI}}$, $\boldsymbol{r}^{\mathrm{WGR}}$, tolerance grid $\{\rho\}$

Ensure: Operational plans, costs, reliability metrics, exposure matrices, divergence statistics

Normalize risk metrics: $R_\star^M \leftarrow \sum_{(i,j)\in\mathcal{L}} r_{ij}^M$ for each M
for each tolerance $\rho \in \{0, 20, 40, 60, 80, 100\}\%$ **do**
    Set metric-specific budgets: $R_{\text{tol}}^M(\rho) \leftarrow (\rho/100)\, R_\star^M$
    Optimize under WFPI: $x^{\mathrm{WFPI}} \leftarrow \text{solve}(r{=}r^{\mathrm{WFPI}}, R_{\text{tol}}{=}R_{\text{tol}}^{\mathrm{WFPI}})$
    Optimize under WGR: $x^{\mathrm{WGR}} \leftarrow \text{solve}(r{=}r^{\mathrm{WGR}}, R_{\text{tol}}{=}R_{\text{tol}}^{\mathrm{WGR}})$
    for each solution $x \in \{x^{\mathrm{WFPI}}, x^{\mathrm{WGR}}\}$ **do**
        Evaluate economics: $C(x) \leftarrow C^{\mathrm{uc}} + C^{\mathrm{oc}} + C^{\mathrm{VoLL}}$
        Evaluate reliability: $\eta(x) \leftarrow \text{Served}/\text{Total} \times 100\%$
        Evaluate exposures: $E^{\mathrm{WFPI}}(x)$, $E^{\mathrm{WGR}}(x)$
    end for
    Construct cross-evaluation matrix $\mathsf{M}(\rho)$
    Compute decision divergence $D(\rho)$ and ranking correlation $\tau(\rho)$
end for
Return comprehensive comparison metrics

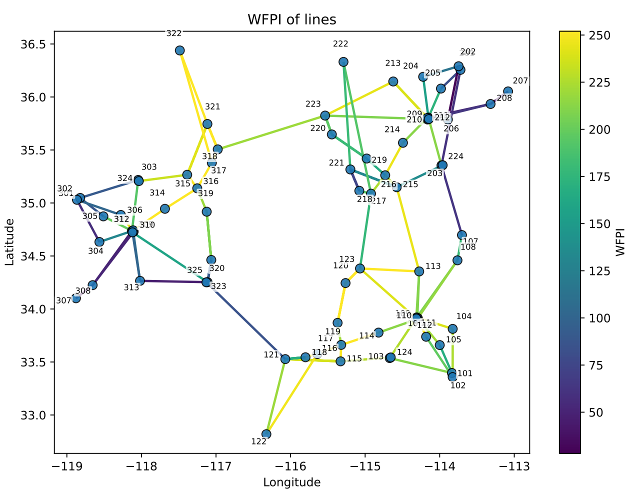

Fig. 1. The RTS-GMLC system with WFPI values.

A. Operating Cost Performance

The results are shown in Table I and Fig. 2. It can be found that the WFPI optimization produces a gradually declining cost curve from \$1.694M at zero tolerance to \$0.684M at full tolerance, requiring 60-80% tolerance to approach baseline operating cost. WGR achieves substantially lower costs under tight constraints, with savings ranging from 51.1% at zero tolerance to 35.0% at 40% tolerance. The WGR cost curve plateaus by 20% tolerance while WFPI requires 60% to narrow the gap, converging fully at 80-100%.

This advantage stems from WGR preserving critical backbone transmission while allocating limited exposure to operationally redundant paths. WFPI de-energizes corridors based on geographic overlap with hazard terrain regardless of operational role, often forcing shutdown of economically critical paths. As tolerance increases, WFPI gradually recovers efficiency by retaining the backbone elements WGR prioritizes.

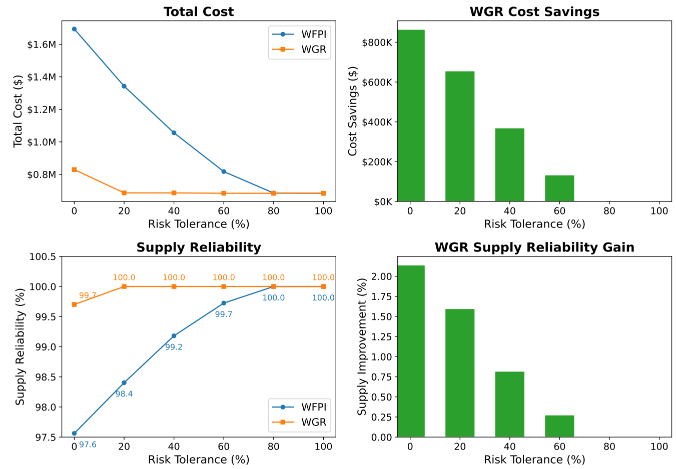

Fig. 2. Comprehensive cross-evaluation across risk tolerances.

TABLE I
COMPREHENSIVE PERFORMANCE METRICS ACROSS RISK TOLERANCES.

Risk Tolerance (%)	Total Cost (\$M) WFPI	WGR	Cost Savings (%)	Reliability Gain (pp)	Decision Divergence (%)
0	1.694	0.829	51.1	+2.1	76.9
20	1.342	0.686	48.9	+1.6	71.8
40	1.056	0.686	35.0	+0.8	56.4
60	0.817	0.684	16.3	+0.3	41.0
80	0.685	0.684	0.2	0.0	20.5
100	0.684	0.684	0.0	0.0	0.0

TABLE II
ZERO-TOLERANCE CROSS-EVALUATION: OPERATIONAL TRADE-OFFS.

Optimization Approach	Total Cost (\$M)	Geographic Exposure	Consequence Risk	Demand Served (%)
WFPI	1.694	0.00	0.00	97.6
WGR	0.829	27.45	0.00	99.7

B. Risk Metrics and Line De-energization Strategies

Table II shows that at zero tolerance, both approaches achieve zero consequence-weighted risk, but through fundamentally opposed strategies. The WFPI plan eliminates all geographic exposure by de-energizing every corridor traversing high-hazard terrain, including backbone paths critical for inter-area power transfer. The WGR plan accepts 27.45 units of geographic exposure concentrated on operationally redundant corridors whose failure would impose minimal system consequences, while preserving backbone infrastructure and achieving 99.7% demand served versus 97.6% under WFPI.

This divergence reflects the imperfect correlation between geographic hazard and system impact. Certain corridors traverse high-WFPI terrain but provide redundant capacity, while

979-8-3315-8138-1

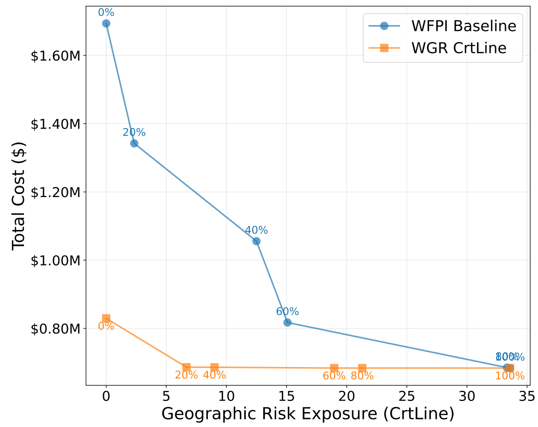

Fig. 3. Cost–exposure Pareto frontiers.

others pass through moderate-hazard zones yet form critical bottlenecks whose loss would trigger cascading curtailments. WFPI treats all exposure equivalently once geographically weighted, whereas WGR prioritizes preserving corridors whose de-energization would cause the greatest unserved energy.

Decision divergence declines monotonically from 76.9% at zero tolerance to 20.5% at 80% tolerance, as expanding risk budgets allow both methods to retain corridors that are simultaneously low-exposure and operationally critical. The monotonicity constraint amplifies early decisions: once de-energized, a corridor remains off throughout the planning horizon, so the high initial divergence propagates across the entire planning period.

In terms of reliability, WGR consistently matches or exceeds WFPI in demand served. The advantage narrows from 2.1 pp at zero tolerance to 0.8 pp at 40% before both methods converge to full service beyond 60%. Under tight constraints, WFPI's geography-driven de-energization isolates load pockets that require costly curtailment, whereas WGR's backbone preservation maintains feasible delivery paths and largely avoids value-of-lost-load penalties, accounting for a substantial portion of the 40–50% cost advantage in the low-tolerance regime.

C. Cost-Exposure Pareto Frontier

Fig. 3 plots total operating cost against geographic exposure. WGR strictly dominates WFPI across nearly the entire feasible range. The WFPI frontier traces a convex curve from $1.694M at zero exposure to $0.684M at full exposure. The WGR frontier exhibits a sharp initial cost reduction followed by a flat region: as minimal exposure is permitted, WGR immediately energizes consequence-critical paths, achieving near-optimal cost. The convergence of frontiers at high tolerance confirms that risk metric selection matters most when constraints bind tightly during extreme fire-weather events.

We note that the DC power flow model used throughout may overestimate backbone transfer capacity in islanded or radial post-PSPS topologies where voltage stability and reactive power become binding. Extending the framework to AC-feasible formulations is a direction for future work.

V. Conclusion

PSPS outcomes hinge on how wildfire risk is defined. Within a unified risk-constrained unit commitment problem, we compare a geographic-exposure index with a consequence-weighted index (WGR) on the RTS–GMLC system. Under tight tolerances, WGR preserves backbone transfers by placing limited exposure on redundant corridors, cutting total cost by 40–50% and increasing served demand by up to 2.1 percentage points; at 0% tolerance the plans disagree on 76.9% of line statuses, and they converge as tolerance relaxes. The framework turns risk tolerance into clear line-level trade-offs and suggests priorities for hardening and operations. Future work includes AC-feasible formulations, time-delayed re-energization models, and decomposition methods for larger networks.

References

[1] N. Rhodes, L. Ntaimo, and L. A. Roald, "Balancing wildfire risk and power outages through optimized power shut-offs," *IEEE Transactions on Power Systems*, vol. 36, no. 4, pp. 3118–3128, 2021.

[2] M. Panteli, P. Mancarella, D. N. Trakas, E. Kyriakides, and N. D. Hatziargyriou, "Metrics and quantification of operational and infrastructure resilience in power systems," *IEEE Transactions on Power Systems*, vol. 32, no. 6, pp. 4732–4742, 2017.

[3] A. M. Stanković, K. L. Tomsovic, F. D. Caro, M. Braun, J. H. Chow, and et al., "Methods for analysis and quantification of power system resilience," *IEEE Transactions on Power Systems*, vol. 38, no. 5, pp. 4774–4787, 2023.

[4] K. W. Hedman, R. P. O'Neill, E. B. Fisher, and S. S. Oren, "Optimal transmission switching with contingency analysis," *IEEE Transactions on Power Systems*, vol. 24, no. 3, pp. 1577–1586, 2009.

[5] X. Liu, M. Shahidehpour, Z. Li, X. Liu, Y. Cao, and Z. Bie, "Microgrids for enhancing the power grid resilience in extreme conditions," *IEEE Transactions on Smart Grid*, vol. 8, no. 2, pp. 589–597, 2017.

[6] Z. Wang and J. Wang, "Self-healing resilient distribution systems based on sectionalization into microgrids," *IEEE Transactions on Power Systems*, vol. 30, no. 6, pp. 3139–3149, 2015.

[7] A. Hussain, V.-H. Bui, and H. M. Kim, "Resilience-oriented optimal operation of networked hybrid microgrids," *IEEE Transactions on Smart Grid*, vol. 10, no. 1, pp. 204–215, 2019.

[8] U.S. Geological Survey, "Understanding wildland fire potential (wfpi): Products and use," https://www.usgs.gov/", 2022, uSGS Fact Sheet; WFPI description and intended use.

[9] N. Rhodes and L. Roald, "Security-constrained optimal power shutoff for wildfire risk mitigation," *IET Generation, Transmission & Distribution*, vol. 18, no. 17, pp. 3326–3337, 2024.

[10] M. Lubin, Y. Dvorkin, and L. Roald, "Chance constraints for improving the security of ac optimal power flow," *IEEE Transactions on Power Systems*, vol. 34, no. 3, pp. 1908–1917, 2019.

[11] E. Dall'Anese, K. Baker, and T. Summers, "Chance-constrained ac optimal power flow for distribution systems with renewables," *IEEE Transactions on Power Systems*, vol. 32, no. 5, pp. 3427–3438, 2017.

[12] C. Barrows, J. Jorgenson, D. Krishnamurthy, J. Lau, G. Stephen, and et al., "The ieee reliability test system: A proposed 2019 update," *IEEE Transactions on Power Systems*, vol. 35, no. 1, pp. 119–127, 2020.

[13] J. H. Scott, J. W. Gilbertson-Day, C. Moran, G. K. Dillon, K. C. Short, and K. C. Vogler, "Wildfire risk to communities: Spatial datasets of landscape-wide wildfire risk components for the united states," Forest Service Research Data Archive, Fort Collins, CO, USA, 2020, updated 25 November 2020. [Online]. Available: https://doi.org/10.2737/RDS-2020-0016

[14] S. Vahedi, J. Zhao, B. J. Pierre, B. Wang, and J. Yusuf, "Probabilistic resilience-oriented assessment approach for transmission networks under wildfires," *IEEE Transactions on Power Systems*, 2025, early access.

979-8-3315-8138-1